Research Article Vol. 13, No. 3 / March 2025 / Photonics Research 611

PHOTONICS Research

Self-injection locked laser via a hollow-core fiber Fabry–Perot resonator

Zitong Feng,[1,2] Meng Ding,[1,*] Matěj Komanec,[3] Stanislav Zvánovec,[3] Ailing Zhong,[3] Francesco Poletti,[1] Giuseppe Marra,[2] and Radan Slavík[1]

[1]Optoelectronics Research Centre, University of Southampton, Southampton, SO17 1BJ, UK
[2]National Physical Laboratory, Teddington, TW11 0LW, UK
[3]Czech Technical University in Prague, Prague 6, 160 00, Czech Republic
*Corresponding author: meng.ding@soton.ac.uk

Received 11 December 2024; revised 11 December 2024; accepted 16 December 2024; posted 17 December 2024 (Doc. ID 530157); published 24 February 2025

In a hollow-core fiber (HCF), light propagates through an air/vacuum core rather than a solid material, resulting in a low thermo-optic coefficient and ability to handle high powers. Here, we demonstrate a laser locked to a hollow-core fiber reference, which thanks to the low HCF thermal sensitivity, shows long-term stability an order of magnitude better than compact commercially available low-noise lasers. The laser frequency variation within ±600 kHz was measured over 50 h. The stability of our proof-of-concept laser is ensured via a strong self-injection ratio of −15 dB, enabled by the high-power handling and low loss of the hollow-core fiber's resonator. Moreover, our results show appealing performance parameters, including a fractional frequency stability of 4×10^{-13} at 1 s averaging time and a Lorentzian component of the linewidth of 0.2 Hz.

https://doi.org/10.1364/PRJ.530157

1. INTRODUCTION

Highly stable lasers are desired in a range of field applications, including high-accuracy lidars [1], relativistic geodesy [2], distributed seismic sensing [3], microwave generation [4], and inertial navigation [5]. Besides practical aspects such as small size, weight, power consumption, and cost, they need to show high stability over short (<1 s) as well as long (>1 s) time scales.

Laser stability is usually improved by locking it to an optical resonator or a delay line. The achievable noise suppression is proportional to the signal delay generated by the resonator or delay line, characterized by the Q factor [6]. Once the Q factor and signal-to-noise ratio (SNR) are high enough, the laser performance is limited by the stability of the resonator or the delay line [6].

The resonator stability is limited by a range of effects, most of them related to temperature variations. At short time scales, dominant noise sources are the thermo-conductive noise [7] that depends on the material thermo-optic coefficient and thermo-refractive noise caused by coupling between the laser's relative intensity noise and material refractive index through the thermo-optic coefficient. At long time scales, the delay line or interferometer delay changes with the waveguide/fiber refractive index drift due to ambient temperature variations, again through the material thermo-optic coefficient. Thus, making the delay line or interferometer from a waveguide with a low thermo-optic coefficient is beneficial on both short and long time scales.

Excellent short-term stability, characterized by frequency noise and Allan deviation at averaging times below 1 s, has been reported in systems based on optical fibers or integrated optics. Fiber-based systems include optical fiber delay lines [8] and optical fiber resonators [9,10]. Outstanding results reported using integrated optics include coil resonators [11], whispering gallery mode resonators [12], spiral resonators [6], and ring resonators [13,14]. Many of these systems demonstrated short-term noise limited by the thermo-refractive noise [7], while long-term stability is typically not discussed, likely to be compromised by the thermo-optic effect in the resonator material, which would require an unpractical (sub-mK) level of temperature stabilization over long time scales. Addressing this would require waveguides with a reduced thermo-optic coefficient or using designs with reduced sensitivity to temperature variations.

Hollow-core fibers (HCFs) have a thermo-optic coefficient of 0.3 ppm/°C (ppm, parts per million) [15], which is significantly lower than for optical materials used for light guiding such as silica (8 ppm/°C) [16] or Si_3N_4 (10 ppm/°C) [11]. This is because light transmitted through the hollow core, as opposed to the transmission through the silica core fiber or

integrated optics waveguide material, avoids most of the light-material interactions. Besides a low thermo-optic coefficient, HCFs exhibit exceptionally low nonlinearity (two to three orders of magnitude lower than silica core fibers). Consequently, HCF can transmit kW-level powers [17], compared to mW levels in integrated optics or μW input powers in high-Q integrated optics resonators, in which the resonant power builds up, causing unwanted Kerr nonlinearities to occur at such low input powers [18]. Lower input power than described above used to avoid nonlinearities may negatively impact the noise of a laser locked to an optical resonator or a delay line, as it may result in a low SNR of the error signal for locking techniques such as in Pound–Drever–Hall (PDH) locking [19]. It can also negatively impact lasers locked using self-injection [20], where low power may cause a reduced locking range, limiting the robustness of the locking to environmental changes.

Here, we demonstrate a laser self-injection locked to an HCF-based Fabry–Perot resonator (HCF-FP). Thanks to the HCF's low thermo-optic coefficient, long-term stability is an order of magnitude better than for commercially available low-noise lasers, with frequency variation within ±600 kHz measured over 50 h. Self-injection locking provides simplicity compared to other phase-locking techniques, such as PDH laser stabilization. Furthermore, using HCF-FP as opposed to HCF delay line allows for a significantly shorter length to achieve the same Q. On short time scales, we achieved a fractional frequency stability of 4×10^{-13} at 1 s averaging time and a Lorentzian component of the linewidth of 0.2 Hz.

2. SELF-INJECTION LOCKED LASER

First, we conducted simulations to evaluate the expected performance of the self-injection locked (SIL) laser shown in Fig. 1. In these simulations, we considered two noise contributions: (i) from the free-running laser after self-injection locking (referred to as SIL noise) [9], and (ii) from the thermo-conductive noise in the HCF-FP [21]. Further, we considered parameters of the components used in experiment. This included a 1550 nm low-cost discrete-mode semiconductor laser from Eblana Photonics, Ireland [22] with 5 dBm output optical power coupled into a single-mode fiber (SMF). A compact polarization controller (OZ Optics) was placed in front of HCF-FP to adjust the input state of polarization. Polarization stability can be well-maintained over several days due to the excellent polarization purity of HCF [23]. Light transmitted through the HCF-FP with power of −10 dBm was injected back into the laser. Given the laser emitted power of 5 dBm and the injected power of −10 dBm, the optical injection locking ratio was −15 dB. This is significantly higher than possible in self-injection locked lasers based on integrated optics resonators [11–13,18] (due to the above-discussed power handling limitations), ensuring robust and stable injection locking [24]. Simultaneously, it is low enough to prevent nonlinear optical injection locking regimes [22]. This makes the used injection power close to the optimum value for our application.

In terms of the HCF-FP, we considered HCF with attenuation of 0.17 dB/km and finesse of 300, which are experimentally achievable values for our all-fiber HCF-FP [25].

For SIL noise calculation, we employed the model described in Ref. [9]. The model requires knowledge of the free-running laser's frequency noise, which we measured (shown later in Fig. 7) and fitted, obtaining $1.4 \times 10^{10}/f^{1.3} + 15000$. Further, we assumed a Q factor of 2.5×10^4. This was obtained by supposing the front laser mirror reflectivity of 50% and laser length of 1.5 mm, which are typical values for discrete mode semiconductor lasers. For the thermo-conductive noise, we considered the HCF parameters shown in Ref. [21].

Calculated SIL noise and thermo-conductive noise contributions considering HCF-FP with lengths of 0.3, 3, and 30 m are shown in Fig. 2(a). SIL noise shows $1/f$ contribution up to a turning point (15, 80, and 200 kHz for 30, 3, and 0.3 m long HCF-FP, respectively), from which it increases.

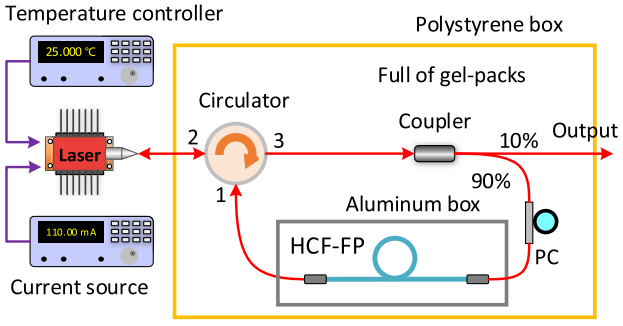

Fig. 1. Schematic of the self-injection locked laser via the HCF-FP. A compact polystyrene box is filled with gel-packs that have a large thermal capacity, passively reducing temperature fluctuations.

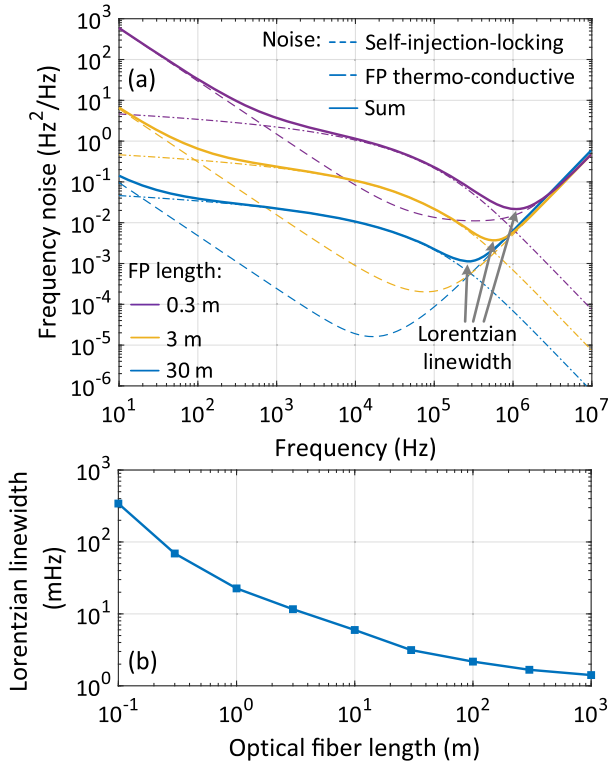

Fig. 2. (a) Simulated frequency noise spectrum when considering self-injection locking noise and thermal noise. (b) Lorentzian linewidth as a function of the HCF-FP length.

Importantly, its level reduces with the square of the HCF-FP length. Thermo-conductive noise also reduces with HCF-FP length, although only linearly. Subsequently, the sum of both noises reduces with increasing HCF-FP length, suggesting longer HCF-FP should reduce the noise, scaling between linear noise reduction (when limited by thermo-conductive noise) and quadratic (when limited by SIL noise).

Figure 2(a) also shows the frequency noise minimum level obtainable with the considered HCF-FPs, which gives the Lorentzian linewidth of the laser. This linewidth is plotted in Fig. 2(b).

Although the above analysis suggests that the longest-possible HCF-FP should give the lowest noise, we decided to use a length of 30 m, as a larger length is associated with a smaller free spectral range and thus also a higher likeliness of mode hopping.

The all-fiber HCF-FP configuration we used is described in detail in Ref. [26] and is shown in Fig. 3(a). It consists of a 29.4 m HCF, aligned and glued with input and output single-mode fibers (SMFs) that have a short segment of graded index (GRIN) fiber spliced on their ends to adapt the mode field from the SMF (10.4 μm at 1550 nm) to that of the used HCF (24 μm at 1550 nm) with dielectric mirrors featuring reflectivity of 99.2%, which are deposited on the SMF end-faces to form the FP cavity. As for HCF, we used double nested antiresonant HCF (DNANF) as opposed to simple nested antiresonant nodeless HCF (NANF) used in Refs. [25,26], which has a lower achievable loss (minimum demonstrated of 0.11 dB/km [27] for DNANF versus 0.22 dB/km for NANF [28], both at 1550–1600 nm). It also exhibits a smaller bend loss, allowing for a tighter coiling and, thus, a reduction in the size of our self-injection locked laser. Figure 3(b) shows the set-up for measuring its transmission using a narrow-linewidth laser (RIO, LUNA). A fiber polarization controller is used to match laser polarization to one set of polarization modes of HCF-FP. The laser's frequency is swept by a ramp wave with a period of 500 ms, and the signals are captured by PDs on an oscilloscope. The frequency sweep speed of 1 MHz over 10 ms enabled us to re-calculate the obtained traces into wavelength, shown in Fig. 4. Figure 4(a), which shows transmission over several HCF-FP

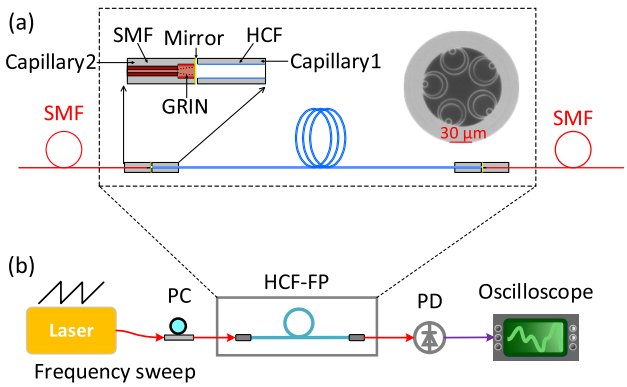

Fig. 3. (a) Schematic of the fabricated HCF-FP. Insert shows a microscope image of the used HCF (DNANF). (b) The set-up to measure the transmission signals of the HCF-FP. PC, polarization controller; PD, photodetector.

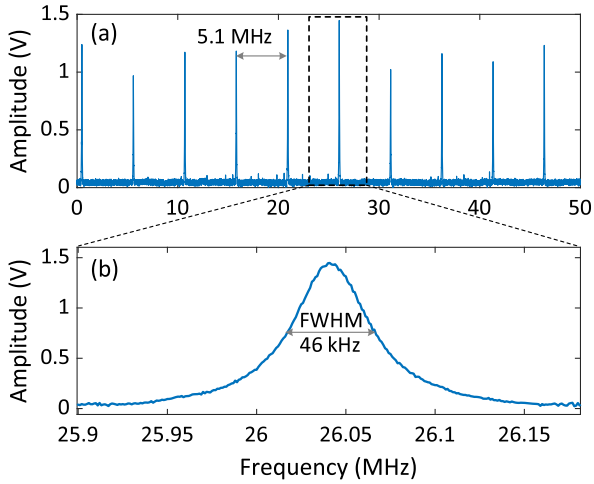

Fig. 4. Transmitted signal through the HCF-FP measured in the set-up shown in Fig. 2(b). (a) Transmission over 50 MHz; (b) detail of transmission of single peak.

peaks, shows the free spectral range of 5.1 MHz, which corresponds to the HCF-FP length of 29.4 m. The uneven transmission spectrum (30% variation between lowest and highest peaks) makes the stable self-injection without mode hops, as the laser self-injection locks on the highest peak within the locking range. Figure 4(b) then shows details of a single transmission peak, showing full width at half maximum (FWHM) of 46 kHz. These values enable to calculate finesse that was 110 and Q factor that was over 4 billion at 1550 nm.

Although we have not actively stabilized the HCF-FP, we have implemented basic passive stabilization, shown in Fig. 1. We have taped the HCF-FP onto an aluminum plate and placed it inside a polystyrene box (wall thickness of 2.5 cm) into which we inserted several gel-packs. The polystyrene box reduced the energy exchange, while the gel packs, with their large heat capacity, increased the amount of energy needed to change the temperature. The temperature fluctuation inside the box monitored by a thermistor changed by up to ±10 mK during our measurement period, which is a level of variation achievable using high-quality temperature controllers and about 50 times better than achievable using a low-cost temperature controller (±0.5 K). In addition, to further reduce the temperature effect to the whole loop of a self-injection locked laser, the total length of SMF is kept to below 0.7 m.

3. MEASUREMENT SET-UPS

Figure 5 shows the experimental set-ups for long- [Fig. 5(a)] and short- [Fig. 5(b)] term characterization of the self-injection locked laser in terms of frequency error and Allan deviation [Fig. 5(a)] and frequency noise [Fig. 5(b)].

The long-term frequency error, Fig. 5(a), was measured by beating the self-injection locked laser with a carrier-envelope-offset stabilized (CEO stabilized) optical frequency comb (OFC). The OFC was stabilized to a ULE-cavity stabilized laser (Menlo, ORS-Compact) for long-term accuracy. We used a 1 nm optical band pass filter to avoid saturation of the photodetector without needing to reduce the power of the comb tone

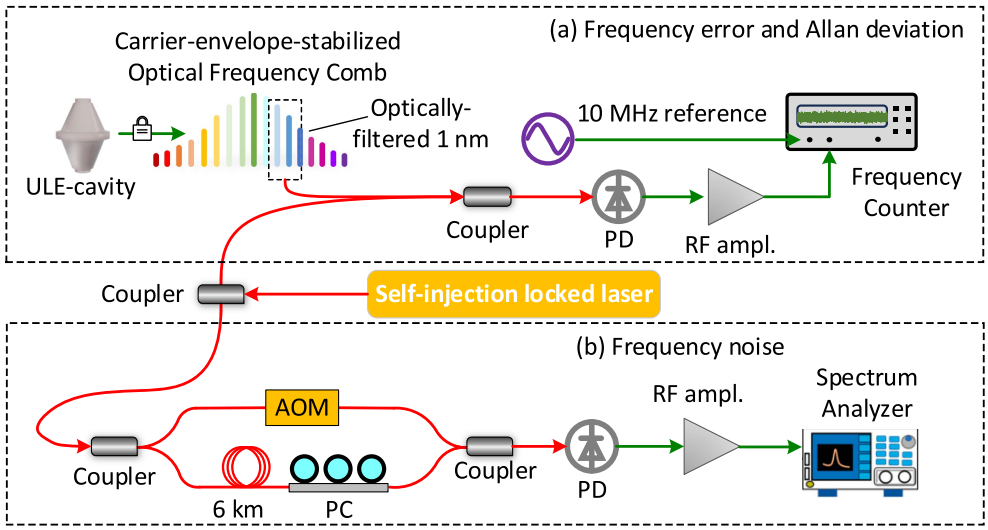

Fig. 5. (a) Experimental set-up for long-term frequency error measurement; (b) optical frequency discriminator set-up for frequency noise measurement. PC, polarization controller; PD, photodetector.

that is needed for beating with the laser. The beat frequency was subsequently amplified and compared to an RF synthesizer locked to a low-noise 10 MHz reference with a zero dead time frequency counter (K + K) with the gate time set to 1 s.

Figure 5(b) shows the frequency noise measurement using an optical frequency discriminator [9]. The laser signal was split by a coupler, with one branch passing through an acousto-optic modulator (AOM) that shifted the frequency by 40 MHz and the other traveling through a 6 km SMF delay line with a polarization controller to optimize interference contrast. The detected 40 MHz beat signal was analyzed using an SA44B spectrum analyzer with built-in phase noise software. The 6 km SMF-based optical delay line enabled measurement up to 10 MHz offset from the carrier when the frequency discriminator sine transfer function was calibrated [9].

4. EXPERIMENTAL RESULTS

A. Frequency Error and Allan Deviation

To demonstrate robustness of our self-injection locked laser, we measured it over 50 h; see Fig. 6(a). During this time, the laser stayed locked without any mode hops. The carrier frequency variations were within ±600 kHz. This variation could be caused by day/night temperature fluctuations in the laboratory, but also by pressure or humidity variations. We believe it could be reduced by placing the HCF-FP into a sealed box and implementing active temperature stabilization.

To appreciate how the achieved level of stability is influenced by the thermal sensitivity of the resonator used for stabilization, we also show results reproduced from Ref. [29], where the stability of a delay line made of SMF was measured over an extended period of time with temperature fluctuations similar to those observed in our experiment (±10 mK). Although the SMF was placed in vacuum (reducing the effects of pressure and humidity variations), it shows frequency excursions that are an order of magnitude larger than those observed with HCF-FP, as would be expected from the difference in thermal sensitivities of the SMF and HCF.

Allan deviations calculated from the data shown in Fig. 6(a) are presented in Fig. 6(b) together with data from manufacturers for RIO [30], BasiK [31], and OEwaves [32] low-noise lasers. Here, we see that the HCF-FP self-injection locked laser achieved about an order of magnitude lower Allan deviation at averaging times beyond 100 s. This was achieved thanks to the HCF's low thermal sensitivity. We expect even better results to be achieved with HCF-FP when its thermal sensitivity is further reduced, e.g., by winding it on a low-thermal-expansion [33] or negative thermal expansion drum [34].

By using an active vibration isolation platform (Accurion Nano 30) to eliminate most of the vibration noise from 1 Hz to 100 Hz, the Allan deviation of 4×10^{-13} at 1 s was achieved [Fig. 6(b)]. This is two to three orders of magnitude better than for commercially available low-noise lasers [30–32], as shown in Fig. 6(b).

B. Frequency Noise and Linewidth

We performed the frequency noise measurement using the set-up shown in Fig. 5(b). First, the performance via a strong injection ratio of −15 dB is demonstrated in Fig. 7 together with the frequency noise of the free-running laser. The measurement noise floor is obtained by removing the 6 km fiber spool. Between 100 kHz and 1 MHz offset frequencies, the frequency noise of the self-injection locked laser reached 0.065 Hz^2/Hz, corresponding to a Lorentzian linewidth of 0.2 Hz. This is over five orders of magnitude lower than that of the free-running laser.

Further, we measured the frequency noise of the self-injection locked laser with different injection ratios (Fig. 8). The results show that the reduction of frequency noise of a laser at Fourier frequency higher than 10 kHz is related to the injection ratio to the laser; the stronger the feedback, the higher the noise suppression. Although the performance degraded when using weaker injection, the Lorentzian linewidth remained as low as 0.3 Hz when the injection ratio was −20 dB, and 1.6 Hz when the injection ratio reduced to −30 dB.

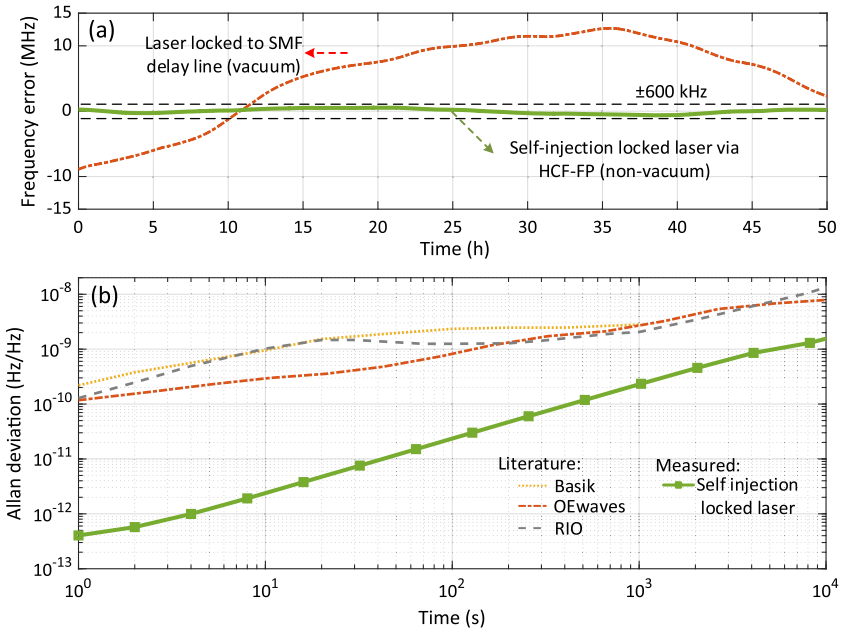

Fig. 6. (a) Frequency error as a function of time achieved here and its comparison with the stability of a laser locked to an SMF delay line placed in a vacuum [29]. (b) Allan deviation calculated from the data shown in (a) and its comparison to measurements reported by manufacturers of commercially available narrow-linewidth lasers [30–32], including OEwaves, which are also based on self-injection locking.

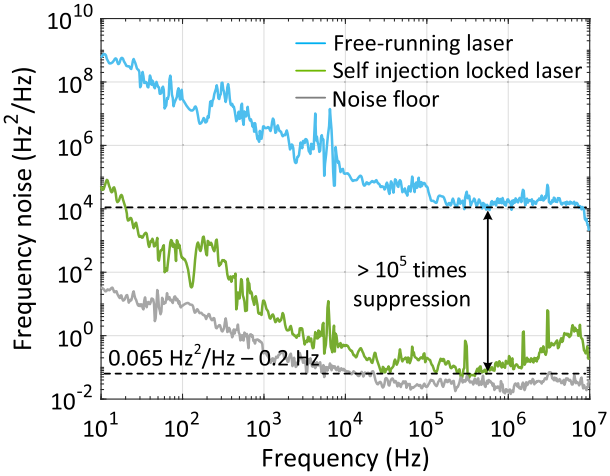

Fig. 7. Measured frequency noise via strong self-injection ratio of −15 dB, together with free-running laser and measurement noise floor.

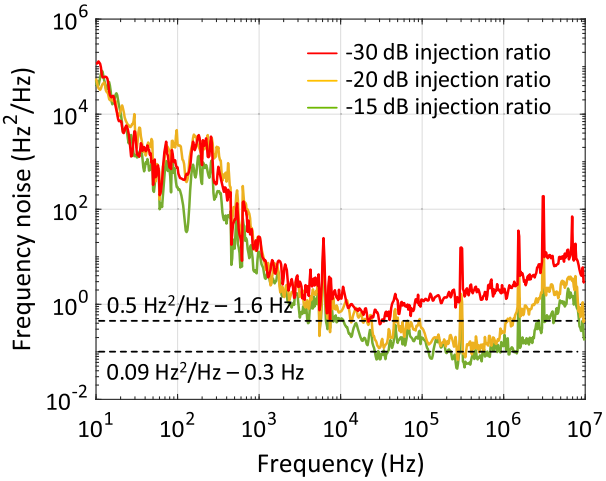

Fig. 8. Measured frequency noise with different self-injection ratios.

Figure 9 shows a comparison of the measured phase noise for injection ratios of −15 and −30 dB with that simulated using the earlier-introduced simulation approach. We see that a higher injection ratio is expected to improve results by 15 dB below 1 kHz offset frequency; however, experimental results are almost identical, suggesting we are limited by other sources of noise in this region, most likely noise due to environmental pick-up in the HCF. The experimentally observed difference in frequency noise of two injection ratios for frequencies above 10 kHz agrees reasonably well with the simulations. However, the simulated level is >10 dB lower than that obtained experimentally, except for frequencies above 1 MHz. Having a model that reasonably predicts performance changes with the injection ratio, but showing different levels of performance suggests the system parameters in the simulation model may require some further tuning, e.g., those describing the laser parameters.

Finally, we measured the relative intensity noise (RIN) performance of the free-running and self-injection locked lasers to rule out possible degradation due to the SIL process as shown in Fig. 10. We can see that RIN is short-noise-limited above 200 kHz with no obvious degradation due to self-injection locking at lower frequencies.

5. DISCUSSION AND CONCLUSIONS

We have demonstrated a self-injection locked laser via an HCF-based resonator with long-term stability (>100 s) an order of

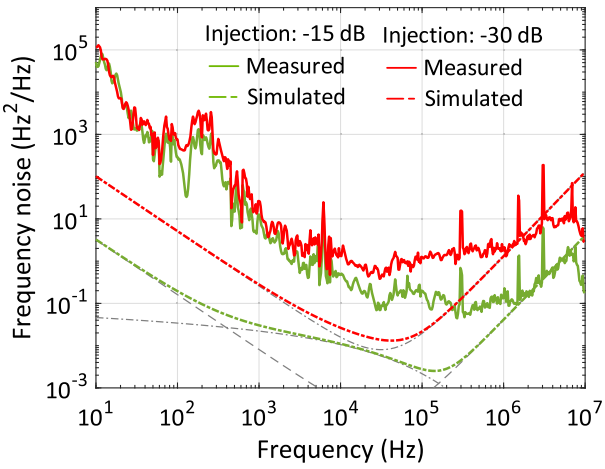

Fig. 9. Comparison of the measured and simulated frequency noise for injection ratio of −15 dB (green) and −30 dB (red). Dashed gray lines show the thermo-conductive noise (which is the same for both cases) and noise contribution due to the self-injection locking.

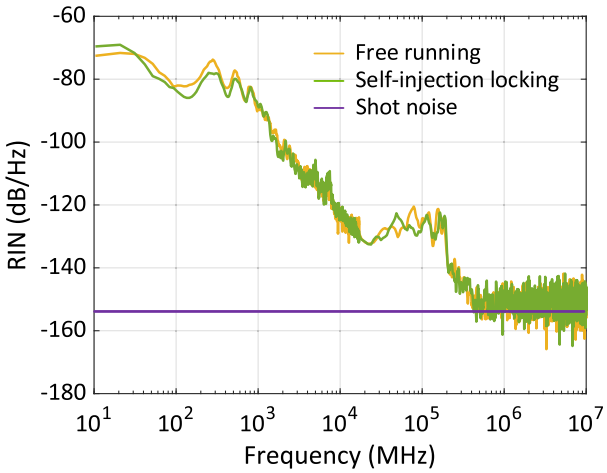

Fig. 10. RIN of the free running and SIL lasers. Shot noise expected for 0 dBm power output is also shown.

magnitude better than low-noise commercially available lasers. We continuously operated the laser over 50 h and achieved laser frequency variation within ±600 kHz. Given its relatively simple configuration and operation in a non-vacuum environment, we anticipate it could be engineered into a small footprint with low power consumption.

We expect that better long-term stability could be achieved with HCF-FP when its thermal sensitivity is further reduced, e.g., by winding it on a low-thermal-expansion [33] or even a negative thermal expansion drum [34].

In the short-term performance, we achieved 0.2 Hz Lorentzian linewidth and Allan deviation of 4×10^{-13} at 1 s averaging time. This is about two to three orders of magnitude better than in commercially available low-noise lasers, one order of magnitude better than with integrated optics resonators [10–12], and is comparable to the SMF delay line with better-performing, but more complex, PDH locking [35].

HCFs exhibit low attenuation across a broad spectral range, from 660 nm (2.9 dB/km [36]) through 1064 nm (0.5 dB/km [36]) and 1550 nm (0.11 dB/km [26]) to 2000 nm (1 dB/km [37]). This will enable self-injection locked lasers across a wide spectral range for applications such as laser spectroscopy and portable optical clocks, covering various atomic transitions. As HCF-FP combines large delay capabilities, low nonlinearity, and low thermal sensitivity, it is a promising platform for the next generation of stabilized laser systems.

Funding. Engineering and Physical Sciences Research Council (EP/P030181/1); VACUUM (EP/W037440/1); Technology Agency of the Czech Republic (FW03010171).

Disclosures. The authors declare no conflicts of interest.

Data Availability. The data underpinning the research presented are accessible through the University of Southampton research repository (DOI: 10.5258/SOTON/D3335').

REFERENCES

1. O. Lux, D. Wernham, P. Bravetti, *et al.*, "High-power and frequency-stable ultraviolet laser performance in space for the wind lidar on Aeolus," Opt. Lett. **45**, 1443–1446 (2020).
2. J. Grotti, S. Koller, S. Vogt, *et al.*, "Geodesy and metrology with a transportable optical clock," Nat. Phys. **14**, 437–441 (2018).
3. G. Marra, D. Fairweather, V. Kamalov, *et al.*, "Optical interferometry–based array of seafloor environmental sensors using a transoceanic submarine cable," Science **376**, 874–879 (2022).
4. T. M. Fortier, M. S. Kirchner, F. Quinlan, *et al.*, "Generation of ultra-stable microwaves via optical frequency division," Nat. Photonics **5**, 425–429 (2011).
5. R. Caldani, S. Merlet, F. Pereira Dos Santos, *et al.*, "A prototype industrial laser system for cold atom inertial sensing in space," Eur. Phys. J. D **73**, 248 (2019).
6. H. Lee, M.-G. Suh, T. Chen, *et al.*, "Spiral resonators for on-chip laser frequency stabilization," Nat. Commun. **4**, 2468 (2013).
7. C. Hilweg, D. Shadmany, P. Walther, *et al.*, "Limits and prospects for long-baseline optical fiber interferometry," Optica **9**, 1238–1252 (2022).
8. F. Kéfélian, H. Jiang, P. Lemonde, *et al.*, "Ultralow-frequency-noise stabilization of a laser by locking to an optical fiber-delay line," Opt. Lett. **34**, 914–916 (2009).
9. L. Hao, X. Wang, D. Guo, *et al.*, "Narrow-linewidth self-injection locked diode laser with a high-*Q* fiber Fabry–Perot resonator," Opt. Lett. **46**, 1397–1400 (2021).
10. S. M. Ousaid, G. Bourcier, A. Fernandez, *et al.*, "Low phase noise self-injection-locked diode laser with a high-*Q* fiber resonator: model and experiment," Opt. Lett. **49**, 1933–1936 (2024).
11. K. Liu, N. Chauhan, J. Wang, *et al.*, "36 Hz integral linewidth laser based on a photonic integrated 4.0 m coil resonator," Optica **9**, 770–775 (2022).
12. W. Liang, V. Ilchenko, D. Eliyahu, *et al.*, "Ultralow noise miniature external cavity semiconductor laser," Nat. Commun. **6**, 7371 (2015).
13. W. Jin, Q.-F. Yang, L. Chang, *et al.*, "Hertz-linewidth semiconductor lasers using CMOS-ready ultra-high-Q microresonators," Nat. Photonics **15**, 346–353 (2021).
14. J. Liu, G. Huang, R. N. Wang, *et al.*, "High-yield, wafer-scale fabrication of ultralow-loss, dispersion-engineered silicon nitride photonic circuits," Nat. Commun. **12**, 2236 (2021).
15. B. Shi, H. Sakr, J. Hayes, *et al.*, "Thinly coated hollow core fiber for improved thermal phase-stability performance," Opt. Lett. **46**, 5177–5180 (2021).

16. R. Slavík, G. Marra, E. N. Fokoua, *et al.*, "Ultralow thermal sensitivity of phase and propagation delay in hollow core optical fibres," Sci. Rep. **5**, 15447 (2015).
17. H. Mulvad, S. Abokhamis Mousavi, V. Zuba, *et al.*, "Kilowatt-average-power single-mode laser light transmission over kilometre-scale hollow-core fibre," Nat. Photonics **16**, 448–453 (2022).
18. K. J. Vahala, "Optical microcavities," Nature **424**, 839–846 (2003).
19. E. D. Black, "An introduction to Pound–Drever–Hall laser frequency stabilization," Am. J. Phys. **69**, 79–87 (2001).
20. L. Wei and Y. Liu, "Compact sub-hertz linewidth laser enabled by self-injection lock to a sub-milliliter FP cavity," Opt. Lett. **48**, 1323–1326 (2023).
21. V. Michaud-Belleau, E. N. Fokoua, P. Horak, *et al.*, "Fundamental thermal noise in antiresonant hollow-core fibers," Phys. Rev. A **106**, 023501 (2022).
22. Z. Zhong, D. Chang, W. Jin, *et al.*, "Intermittent dynamical state switching in discrete-mode semiconductor lasers subject to optical feedback," Photon. Res. **9**, 1336–1342 (2021).
23. A. Taranta, E. N. Fokoua, S. A. Mousavi, *et al.*, "Exceptional polarization purity in antiresonant hollow-core optical fibres," Nat. Photonics **14**, 504–510 (2020).
24. Z. Liu and R. Slavík, "Optical injection locking: from principle to applications," J. Lightwave Technol. **38**, 43–59 (2020).
25. M. Ding, E. R. N. Fokoua, T. D. Bradley, *et al.*, "Finesse limits in hollow core fiber based Fabry-Perot interferometers," J. Lightwave Technol. **39**, 4489–4495 (2021).
26. M. Ding, M. Komanec, D. Suslov, *et al.*, "Long-length and thermally stable high-finesse Fabry-Perot interferometers made of hollow core optical fiber," J. Lightwave Technol. **38**, 2423–2427 (2020).
27. Y. Chen, M. N. Petrovich, E. N. Fokoua, *et al.*, "Hollow core DNANF optical fiber with <0.11 dB/km loss," in *Optical Fiber Communication Conference* (Optica Publishing Group, 2024), paper Th4A.8.
28. H. Sakr, T. D. Bradley, G. T. Jasion, *et al.*, "Hollow core NANFs with five nested tubes and record low loss at 850, 1060, 1300 and 1625 nm," in *Optical Fiber Communication Conference* (Optica Publishing Group, 2021), paper F3A.4.
29. I. B. Edreira, R. Slavík, J. K. Sahu, *et al.*, "Frequency drift characterization of a laser stabilized to an optical fiber delay line," Opt. Express **32**, 16823–16830 (2024).
30. L. Stolpner, "Planar external cavity low noise narrow linewidth lasers," in *PDV Workshop* (2011).
31. J. E. Pedersen, "Low noise frequency stable fiber lasers for optical remote sensing application," in *PDV Workshop* (2012).
32. W. Liang, V. S. Ilchenko, D. Eliyahu, *et al.*, "Compact stabilized semiconductor laser for frequency metrology," Appl. Opt. **54**, 3353–3359 (2015).
33. M. Ding, E. N. Fokoua, J. R. Hayes, *et al.*, "Hollow-core fiber Fabry–Perot interferometers with reduced sensitivity to temperature," Opt. Lett. **47**, 2510–2513 (2022).
34. I. B. Edreira, M. Ding, B. Shi, *et al.*, "Thermal properties of a hollow-core optical fiber spooled onto a drum with negative coefficient of thermal expansion," in *IEEE Photonics Conference (IPC)* (IEEE, 2023), pp. 1–2.
35. I. Jeon, C. Ahn, C. Kim, *et al.*, "Palm-sized, vibration-insensitive, and vacuum-free all-fiber-photonic module for 10^{-14}-level stabilization of CW lasers and frequency combs," APL Photon. **8**, 120804 (2023).
36. H. Sakr, Y. Chen, G. T. Jasion, *et al.*, "Hollow core optical fibres with comparable attenuation to silica fibres between 600 and 1100 nm," Nat. Commun. **11**, 6030 (2020).
37. X. Zhang, W. Song, Z. Dong, *et al.*, "Low loss nested hollow-core antiresonant fiber at 2 μm spectral range," Opt. Lett. **47**, 589–592 (2022).